# Two-photon polymerization for biological applications

Alexander K. Nguyen<sup>a</sup>, Roger J. Narayan<sup>a</sup>

 ${\it aUNC/NCSU Joint Department of Biomedical Engineering, North \ Carolina \ State \ University,}$ 

Raleigh, NC 27695-7115 USA

Corresponding author:

Roger J. Narayan

UNC/NCSU Joint Department of Biomedical Engineering

Raleigh, NC 27695-7115 USA

T: 1 919 696 8488

E: roger\_narayan@unc.edu

#### Abstract

Two-photon polymerization (2PP) leverages the two-photon absorption (TPA) of near-infrared (NIR) radiation for additive manufacturing with sub-diffraction limit resolution within the bulk of a photosensitive material. This technology draws heavily on photosensitive polymers from the microelectronics industry, which were not optimized for TPA or for biocompatibility. 2PP with sub 100 nm resolution has been repeatedly demonstrated; however, this level of fabrication resolution comes at the expense of long fabrication times. Manufacturing of medical devices beyond surface texturing would be prohibitively slow using the current state of the art 2PP technology. Current research into TPA-sensitive photopolymers with good biocompatibility and holographic projections using spatial light modulators address current technological limitations by providing materials specifically formulated for biological applications and by making better use of available laser power for applications in which nanoscale resolution is not required. respectively.

## Keywords

additive manufacturing; two-photon polymerization; spatial light modulator; photopolymerization

#### Introduction

Additive manufacturing (AM) techniques are freed from many of the practical concerns associated with incumbent fabrication techniques such as computerized numerical control (CNC) milling; however, additive manufacturing techniques commonly face limitations associated with the tool path. For example, in ultraviolet light-based stereolithography (SLA), light as the "tool" is "bound" by its interaction with the photopolymer surface. For this reason, AM techniques are often described as "layer-by-layer" techniques. Two-photon polymerization (2PP) breaks free from this paradigm due to the absence of this tool path limitation. 2PP utilizes the two-photon absorption of near infrared (NIR) light to excite the same energy transition as ultraviolet (UV) photons. Since the 2PP photopolymer is transparent to this fundamental wavelength, the 2PP "tool" is essentially an unsupported floating point that is able to process material within the photopolymer. This process is not diffraction limited, allowing for sub-wavelength fabrication; structures with dimensions below 100 nm have been fabricated out of a chemically modified zirconium-based sol-gel composite material using this approach. Just as stereolithography evolved from a laser-scanning approach to a two-dimensional digital-light projection approach, laser-scanning 2PP has the ability to evolve into a three-dimensional holographic projection approach.

The unique capabilities associated with 2PP stem from the capability for sub-micrometer resolution materials processing and from the unsupported voxel; intricate features can be made in regions of structures that are impossible to access using other fabrication techniques. One set of interesting applications of 2PP is fabrication within a microfluidic channel. 2PP-based structuring is performed within a photopolymer-filled channel, followed by exposure to the developing solution. For example, Wu et al. not only generated Fresnel lenses within a microfluidic channel but also fabricated a porous filter, which would have been difficult to conventionally fabricate and place within the channel. The lenses in combination with the filter were used as a white-light cell counter.<sup>2</sup> 2PP was also used to generate porous microchannels for the study of chemotaxis in dendritic cells. The 500 nm pores in the channels generated within the microfluidic channel were too small for the cells to grow into but large enough for transport of the desired chemokine.<sup>3</sup> A 2PP-fabricated hypodermic microneedle was integrated with a microfluidic device; this device was able to uptake solutions containing physiologically-relevant K<sup>+</sup> solutions for detection with an ion-selective electrode.<sup>4</sup> Producing structures on the cellular size scale opens up many opportunities to determine the cellular response to substrate geometry; for example, neuronal cells have been shown to extend neurites along channels with features on the micrometer scale.<sup>5</sup> In another study, a biomimetic scaffold was produced from Ormocomp®, an organically modified ceramic, using computed tomography images of human trabecular bone; good adhesion of SaOS-2 osteoblast-like cells to the scaffold surfaces was demonstrated.<sup>6</sup>

At this time, 2PP is not commonly used for biological applications due to the toxicity of many feedstock materials and the difficulty of producing mesoscale structures that are relevant for biological applications. Since most 2PP polymers have been adopted from established SLA technologies, they were not formulated for either 2PP or biological applications. In addition, the nano-scale precision offered by 2PP is a source of weakness; structures with small-scale features require relatively long fabrication speeds. Strategies such as soft lithography replication of a 2PP-fabricated master structure have been demonstrated<sup>7,8</sup>; however, these strategies are stop gap measures and do not overcome existing weaknesses. Novel photopolymers exhibiting increased 2PP sensitivity and optics that are able to process larger volumes must be developed to enable large-scale commercial translation. In this paper, the excitation mechanisms associated with 2PP, innovations in photosensitive materials for 2PP, and innovations in optical setups for 2PP will be considered.

## **Excitation Mechanisms**

Despite having "two-photon" in its name, 2PP proceeds by multiple mechanisms, only one of which involves two-photon absorption. In the traditional one-photon case, the photoinitiator is excited to a higher singlet state and decays through an intersystem that crosses to the triplet state. Due to this forbidden transition, the triplet state has a much longer lifetime; the long half-life of the

triplet species allows for emission even seconds after excitation. These triplet species can form free radicals, which initiate polymerization; as such, photoinitiator designs having long triplet lifetimes are beneficial to UV lithography and 2PP by extension. Unlike UV lithography, 2PP involves extremely intense laser radiation on the order of terawatts per cm<sup>2</sup>, which is associated with the possibility of multiphoton ionization and subsequent dielectric breakdown.

Dielectric breakdown, also known as avalanche ionization, occurs in regions of highly intense electric fields and causes a normally insulating species to become locally conductive. Electrons in the conduction band of a material can be accelerated by the electric field and transfer energy to other electrons in the valence band, promoting those electrons to the conduction band. These child electrons can also be accelerated, generating conduction band electrons within the laser focus in an exponential manner. Order of magnitude estimations of multiphoton and avalanche ionization that were calculated for SZ2080 zirconium Ormosil®, a photoresist used both for photonics and biological applications, revealed that the contribution from avalanche ionization is much greater than from two-photon absorption near the 2PP threshold.<sup>9</sup> Since dielectric breakdown would also take place within the monomer, it is possible to perform 2PP without this generally toxic compound. Eliminating photoinitiators would be very attractive from a biocompatibility viewpoint; however, the working range of the 2PP process would be severely narrowed.

The working range is informally limited by (a) the 2PP threshold, the average laser power found in practice to initiate polymerization, and (b) the burning threshold, the power at which the material breaks down and generates bubbles that destroy the sample. Dielectric breakdown requires a conductive electron to be accelerated; such electrons are exceedingly rare in insulators and the vast majority of polymers. A photoinitiator with a quasi-stable excited state has multiple seeds for dielectric breakdown.

Malinauskas et al. reported 2PP structuring without a photoinitiator in Ormosil®; the 2PP threshold was cut in one-third and the working range was tripled with addition of 1% by weight Irgacure® 369 or Michler's ketone.

Simple heating of a photopolymer can cause polymerization, which can result in unwanted voxel spread. For example, SU-8, a polymer from the microelectronics industry that is commonly used in biological studies, will thermally polymerize when exposed to temperatures above 167°C.<sup>10</sup> It was calculated that a 0.5 nJ pulse, which approximates the energy from a 50mW Ti:Sapphire laser operating at 80 MHz, would generate an equilibrium temperature of 227°C within the focal volume (assuming insufficient time for heat diffusion).<sup>11</sup> Considering a typical 80 MHz repetition rate and a 1 µm voxel size, the laser focus would have to scan at above 80 m/s to have no voxel overlap. Since 2PP experiments commonly typically take place with scan speeds in the range of millimeters per second, heat-initiated polymerization is a major contributor to the final dimensions of a 2PP-fabricated structure. Baldacchini et al. used a pulse width modulated (PWM) acousto-optical modulator to chop the 80 MHz laser into bursts with variable repetition rates. Decreasing the repetition rate (at a constant average laser power and burst width) increased the resolution of the 2PP-fabricated structures.<sup>12</sup> Although an identical average power is experienced by the sample, allowing the local regions to cool by spacing out the pulses reduces the effect of thermal polymerization.

Drawing multiple lines simultaneously is one method to increase the fabrication speed; this approach is possible with laser technologies but it is associated with voxel spread via diffusion of the polymerization propagating species. Cross-talk between fine features (e.g., diffraction gratings or wave guides) occurs when the scanning process is rapid. Much of this phenomenon can be explained by heat buildup within the substrate; however, a linewidth increase of up to 25% was noted in experiments in which thermal effects were considered negligible. The effects of spatial and temporal proximity were investigated by scanning two foci separated by an x and y distance; when scanning parallel to the y-axis, the x separation constituted spatial separation between the two lines and the y-separation formed the temporal delay. The focus trailing behind the other contained a higher concentration of initiating species, which diffused from the leading pulse and caused broadening. This effect was significant out to 100 ms temporally and 3000 nm spatially, the separation limits associated with the optical beam path. Current fabrication strategies such as raster scanning often involve marking parallel lines spatially and temporally shorter than these values; as such, this "proximity effect" must be considered

when tight tolerances are required.

Since two-photon absorption (TPA) is the mechanism that seeds polymerization, maximizing the TPA coefficient is an important factor in 2PP photopolymer design. In single photon absorption, the intensity of the transmitted light is dependent on the linear absorption coefficient ( $\alpha$ ), concentration, and path length as per the Beer-Lambert law. The non-linear absorption coefficient ( $\beta$ ) becomes a non-negligible factor at high intensities; it can be negative for saturation of absorbance or positive for multi-photon absorbance. This phenomenon is measured using the Z-scan technique, in which a sample is translated along the axis of a converging laser while the transmitted light intensity is measured. In the typical Z-scan apparatus, the non-linear absorption coefficient is measured in an open aperture configuration in which all of the transmitted light is collected; any change in transmittance while scanning through the focus would be due to non-linear (e.g., two-photon absorption) effects. The theoretical calculations behind this technique incorporate three main assumptions to simplify the calculations: 1) only the third-order non-linearity (two-photon processes) are considered, 2) the sample thickness is shorter than the Rayleigh range of the focus, and 3) the laser is a TEM<sub>00</sub> Gaussian beam. If one approximates the sample to be a "thin" sample, then the laser focal region dimensions do not vary significantly within the sample while being translated within the beam. This approach enables use of the slowly varying envelope approximation; higher order differentials in the equation representing electric field can be ignored. Using a Gaussian beam simplifies the calculations since the Fourier transform of a Gaussian distribution is also Gaussian. At the endpoint of the calculations, the change in normalized transmission through the sample can be represented by the Taylor series:

$$T(z) = \sum_{m=0}^{\infty} \frac{[-q_0(z,0)]^m}{(m+1)^{3/2}}$$

Where  $q_0(z,0)$  is:

$$q_0(z,0) = \frac{\beta I_0 L_{eff}}{(1 + \frac{z^2}{Z_R^2})}$$

In this equation,  $z_R$  is the Rayleigh range,  $L_{eff}$  is the effective path length represented by  $L_{eff} = \frac{(1-e^{-\alpha L})}{\alpha}$ , and  $I_0$  is the peak irradiance at the focus of the sample. <sup>14</sup> Since photopolymers used with 2PP should be transparent to the laser radiation,  $\alpha$  will be very small, which makes  $L_{eff} \approx L$ . For a perfectly Gaussian beam,  $I_0$  can be given by <sup>15</sup>:

$$I_o = \frac{4 P_{Avg}}{\pi \omega_0^2 R \tau} \sqrt{\frac{\ln(2)}{\pi}} = \frac{4 P_{Avg}}{M^2 \lambda z_R R \tau} \sqrt{\frac{\ln(2)}{\pi}}$$

where R is the repetition rate,  $\tau$  is the pulse duration,  $\omega_0$  is the beam waist, and  $M^2$  is the beam quality. All parameters in  $I_0$  are either defined by the experimenter (i.e., average power  $P_{avg}$  and Rayleigh length  $z_R$ ) or the characteristics of the laser.  $L_{eff}$  is an experimental parameter, leaving the value for  $\beta$  unknown.  $\beta$ , the non-linear absorption coefficient, can be numerically fit to the Taylor series. Further approximating the value by only considering the m=1 term in the series, using L in place of  $L_{eff}$ , and subtracting the m = 0 term (which is simply 1 in any case), a greatly simplified equation in terms of the change in the normalized transmittance can be obtained:

$$T(z) - 1 = \Delta T(z) = \frac{-\beta I_0 L}{2\sqrt{2}(1 + \frac{z^2}{z_R^2})}$$

Although the highest change in transmittance will always be found at z = 0, noise in the data can make it difficult to find the exact values for  $\Delta T(0)$  and  $z_R$ . An example of a normalized transmission plot is given in Figure 1, which indicates the effect of peak intensity on TPA. That said, a good starting point to qualitatively compare different photoinitiator formulations would be to measure

the relative change in transmittance at z = 0 while accounting for potential differences in the sample path lengths. Finding photoinitiator formulations with high TPA cross-sections generates a list of moieties that are highly efficient absorbers.

## Photopolymer design strategies

Designing an efficient 2PP photoinitiator differs from designing an efficient ultraviolet photoinitiator since the TPA cross-section is not considered during development of an ultraviolet photoinitiator; however, designing an efficient 2PP photoinitiator and designing an efficient ultraviolet photoinitiator share many strategies. In general, high TPA cross-section photoinitiators commonly consist of an extended  $\pi$ -system chromophore that is flanked by multiple electron donating or withdrawing groups. <sup>16,17</sup>Ethyl Michler's ketone is composed of a benzophenone with a diethyl amino group at each of the para- positions. Another consideration is the efficiency of the radical species that initiate polymerization. Furthermore, there must be a bridge between these two criteria in which the excited state can form the radical species. <sup>16</sup>

The mechanism by which the free-radical species is formed splits photoinitiators into two classes. Type 1 photoinitators are cleaved from the triplet state, forming two free radicals that can initiate chain polymerization. In contrast, the triplet excited state of type 2 photoinitiator chromophores must react with a co-initiator, which subsequently forms the radical species. Type 1 photoinitiators are more common since photocleavage is a mono-molecular reaction; type 2 photoinitiators utilize bi-molecular reactions and are less efficient. It should be noted that type 2 photoinitiator formulations in which the chromophore is covalently bonded with the co-initiator allow for formation of a free radical species in a mono-molecular reaction without cleavage.<sup>18</sup>

Considering the TPA cross-section, the mechanism of radical formation, and the initiation efficiency leaves few 2PP feedstock materials with appropriate features for biological applications. Photoinitiators are generally toxic materials since reactive oxygen species are harmful to cellular function. As such, type 1 photoinitiators designed to easily cleave are not the most biocompatible class of materials. For this reason, recent research efforts have been geared toward the development of biocompatible type 2 photoinitiators. For example, high TPA cross-section chromophores (shown in Figure 2) were produced from two different  $\pi$ extended ketocoumarins and modified with different diakylamino- groups; these materials were shown to exhibit 100% cell viability and similar proliferation rates to the glass control. 19 The combination of riboflavin and triethanolamine has been used as a UV photoinitiator<sup>20</sup> and has been successfully used for 2PP.<sup>21</sup> No statistically significant difference in cell viability was noted between riboflavin- triethanolamine wafers and glass. Growth of bovine aortic endothelial cells on a polyethylene glycol-riboflavintriethanolamine scaffold processed using 2PP was demonstrated (Figure 3); a LIVE/DEAD<sup>TM</sup> stain of a five day culture of GM7373 endothelial cells demonstrated a significant number of live cells and few dead cells. It should be noted that riboflavin-triethanolamine was less efficient than conventional photoinitiators (e.g., Irgacure® 369 and Irgacure® 2959) in terms of the laser fluence required for 2PP. The higher laser fluence required for this photoinitiator formulation is affected by the TPA cross section and radical generation from the excited state. While each parameter is important individually, all of the factors can be summed up by the processing window. Qualitatively speaking, the processing window is related to the scanning speed and the laser power, the product of which gives the laser dosage exposed to a volume. A more effective photoinitiator would have a wide range of speed and a power at which good structuring is observed. The gold standard to evaluate the processing window is a parametric study that evaluates each speedpower combination. An example parameter search array is given in Figure 4, in which both parameters are serially tested.<sup>22</sup> In areas with high power and low speed, poor structuring is observed since the polymer burns from the high irradiation. Areas with high speed and low power are underexposed, which results in weak or missing structures. A wide processing window between these two zones indicates an easy-to-use photoinitiator.

Water insoluble photoinitiators make up the majority of available products on the market; however, their insolubility does not rule out their use in hydrogels. Pawar et al. used 2,4,6-trimethylbenzoyl-diphenylphosphene oxide (TPO) as a model water insoluble

photoinitiator to process aqueous acrylamide in an SLA setup. The TPO was prepared as an oil-in-water microemulsion and then spray dried to produce a dry nanoparticle powder; dispersing this powder into water yielded a clear solution.<sup>23</sup> TPO and ethyl Michler's ketone are well established photoinitiators that are also unfortunately water insoluble, preventing their traditional use in hydrogels. Preparing these photoinitiators in nanoparticle form would be one method for photosensitizing hydrogel monomers. Although these materials are not highly biocompatible, post processing steps and the insolubility of these materials would reduce the amount of material that enters the biological environment during use.

Appropriate photopolymers for biological applications would ideally have a high degree of conversion to minimize the amount of residual monomer and fast polymerization kinetics to reduce the required laser dwell time necessary to achieve full polymerization. Being able to tune the mechanical properties and degradation characteristics would be an ideal characteristic for several tissue engineering applications. Biological uses of photopolymers are already commonplace albeit not with photopolymers that are processed using additive manufacturing approaches. Dental applications draw heavily on methacrylates that are commonly initiated by Type II photoinitiators due to their compatibility with visible light; however, Type I photoinitiators may also be used. Further examination of dental photopolymer systems may suggest appropriate methacrylate formulations for use with 2PP.

The Degree of Conversion (DC) determines the final mechanical properties and the biocompatibility of the structure (e.g., the biocompatibility of the structure may be reduced by leaching of unreacted monomer). Changes in Fourier transform infrared spectra (e.g., changes in the vinyl peak) are commonly used to determine the DC value. For example, the DC value for a 55:45 molar ratio of 2,2-bis[4-(2-hydroxy-3-methacryloxypropoxy)phenylpropane (BisGMA) and 2-hydroxyethylmethacrylate (HEMA) mixture was monitored with an Attenuated Total Reflectance FTIR (AT-FTIR). The ratio of the 1637 cm<sup>-1</sup> peak (associated with aliphatic C=C) to the 1608 cm<sup>-1</sup> peak (associated with aromatic C=C) was evaluated. Measurements obtained at multiple times during polymerization were compared to the initial ratio of the monomer solution; these measurements were used to calculate the DC values for the system.<sup>24</sup> This approach was also used to examine a 7:3 mass ratio of BisGMA and triethyleneglycoldimethacrylate (TEGDMA).<sup>25</sup> Both studies evaluated the effect of several photoinitiators and illumination conditions on camphorquinone (CQ)-based photoinitiators. DC values for these systems, which exhibit 20-70% conversion, are heavily influenced by the choice of photoinitiator. Additional photoinitiator systems based on 9,10-phenanthrenequinone (PQ), TPO, and phenylbis(2,4,6-trimethylbenzoyl)phosphine oxide (BAPO) were investigated for a 55:45 BisGMA:HEMA monomer mixture under wet and dry conditions.<sup>26</sup> A study that investigated the reaction kinetics for several ratios of BisGMA and TEGDMA with a CQ-based Type II photoinitiator or a monoacylphosphine (MAPO) Type I photoinitiator showed changes in the DC value from variations in the monomer ratio and the photoinitiator type. The use of MAPO resulted in a higher final DC value, with polymerization requiring one-fourth to one-sixth the amount of time to reach 95% of the final DC value. High performance liquid chromatography analysis of monomer eluted after one week in a 75% ethanol solution revealed a steep slope between the total monomer eluted and the DC value (e.g., 12% by weight eluted at 40% DC versus 3% eluted at 50% DC).<sup>27</sup> Both photoinitiators used in this study are not biocompatible; however, the marked difference between the DC values (and the amount of elutable monomer by extension) raises questions about the trade-off between photoinitiator toxicity and DC value. Since a high DC value is associated with less residual monomer and less toxicity, the effect of laser-material interaction on DC should also be considered. Cica et al. demonstrated 2PP of a 1:1 mixture by weight of trimethylolpropane triacrylate and ethoxylated(20) trimethylolpropane triacrylate, which was photoinitiated by either 2,7-bis[((4-dibutylamino)phenyl)ethynyl]-9 H-fluoren-9-one (B3FL) or E.E-1,4-bis[4'-(N,N-di-n-butylamino)styryl]-2,5-dimethoxybenzene (R1) at a 6.3 µmol/g concentration; several scan speeds and average laser powers were evaluated in this study. The DC values of the 50 µm x 50 µm x 30 µm structures were calculated using data from the 810 cm<sup>-1</sup> peak, which was attributed to carbon double bonds; the carbon double bond data was normalized using data from the 1730 cm<sup>-1</sup> carbonyl peak. Scan speed was found to have an effect on the DC value near the 2PP threshold, the lowest laser power at which polymerization is observed. The correlation between scan speed and DC value was not significant at high power

values; changing the scan speed from 100 to 800 μm/s at the threshold reduced the DC value from 61% to 56%. A DC value of 74% was obtained for structures within this scan speed range when using power values above 1.75x the threshold were utilized.

Hydrogels are commonly polymerized with 2PP since this class of materials is commonly used in studies involving soft tissue regeneration. In addition, several types of biological polymers, including carbohydrate- and protein- based materials, can be modified with photopolymerizable groups to make them feedstock materials for the 2PP process. It is also common to incorporate (a) growth factors or (b) compounds within the polymer chain that alter its mechanical properties. The general procedure for modifying the backbones of synthetic and biological polymers with pre-polymer groups is similar.

The addition of methacrylate groups can be undertaken with glycidyl methacrylate, which can react with carboxyl, hydroxyl, and amine groups to form a corresponding carbonyl linkage that terminates in a methacrylate group. <sup>29,30</sup> Methacrylation of hyaluronic acid using this approach is straightforward due to its water solubility. Chitosan must be modified with succinic anhydride to become soluble in water; reaction with an amine group on the chitosan backbone forms an amide linkage that terminates in a carboxylate group. Incubation of either hyaluronic acid or N-succinylated chitosan with glycidyl methacrylate over ten days yielded a photopolymerizable hydrogel. Purification was performed by precipitation in acetone, dialysis in pure water, and lyophilization. The mechanical properties of the methacrylated polymer can be modified by the addition of polyethylene glycol diacrylate. Lactate dehydrogenase and cell proliferation assays indicated that both the base methacrylated polymer and the copolymer containing polyethylene glycol diacrylate possess biocompatibility similar to that of the tissue culture polystyrene control. <sup>29,30</sup>

A process utilizing the more reactive methacrylic anhydride was described for methacrylation of gelatin; the degree of substitution can be controlled by varying the concentration of the methacrylic anhydride in the solution. The procedure is relatively simple, involving the addition of methacrylic anhydride to a 50°C gelatin solution in phosphate buffered saline over a period of one hour. Dialysis over twenty-four hours and lyophilization completed the purification of the material.<sup>31</sup> 2PP was used to process material into a woodpile-style scaffold; human adipose-derived stem cells were able to proliferate through the structure and differentiate into adipocytes.<sup>32</sup> The reactive methacrylating agent has also been used to modify a biodegradable polylactic acid base polymer with organic solvents.<sup>21</sup> The photopolymer that was obtained using this approach was seeded with a human SH-SY5Y human neuronal cell line and with primary rat Schwann cells.<sup>33</sup>

All of the photopolymers mentioned thus far have been negative photoresists; it should be noted that positive photoresists, for which illumination causes polymer cleaving, are also compatible with multiphoton absorption technology. For example, Kloxin et al. produced a photocleavable PEG-based polymer using 4-[4-(1-hydroxyethyl)-2-methoxy-5-nitrophenoxy]butanoic acid as the photolabile group. The addition of an acrylate group via the alcohol resulted in production of the photodegradable acrylate, the carboxylic acid of which attached to polyethyleneglycol-bis-amine to form the crosslinkable monomer. Ammonium persulfate and tetramethylenediamine were used for radical-mediated polymerization of the bulk polymer. Exposure to 365 nm light, or two-photon excitation by 740 nm light commonly produced by a Ti:sapphire femtosecond laser, caused hydrolysis of the ester group adjacent to the acrylate group. Kloxin et al. also provided a procedure for cell encapsulation within the crosslinked polymer. One important advantage of using a positive photoresist with encapsulated cells is that UV phototoxicity is not be an issue; the cell-laden polymer exposed to in-focus NIR light is washed away during development; the out-of-focus NIR light should have little effect on cells compared to the UV light that is used in traditional lithography.

While not a traditional polymerization reaction, certain proteins can be crosslinked without modification through a complex reaction that involves singlet oxygen generation from a chromophore. Crosslinking of collagen using UV light is well known and is commonly utilized by ophthalmologists for the treatment of keratoconus.<sup>35</sup> A 40% increase in the stiffness of collagen-rich tissue cultured *in vitro* from murine embryonic fibroblasts and neonatal rat cardiomyocytes was demonstrated using this approach.<sup>36</sup> Singlet oxygen can also be generated using TPA from aromatic amino acids within the proteins themselves; this mechanism enables

crosslinking of protein solutions without the inclusion of additional photosensitizers.<sup>37</sup> The addition of a chromophore such as methylene blue, rose bengal, or flavin adenine dinucleotide can improve the crosslinking performance.<sup>38</sup> Robust 3D structures such as small cantilevers or chambers may be processed using this approach. By precisely measuring the mechanical properties of crosslinked avidin structures using atomic force microscopy, Khripin et. al. was able to measure the pressure of proliferating *E. coli* within a chamber; this approach can be potentially used to predict pressures within cancerous tumors.<sup>39</sup>

Tissue engineering of orthopedic implants requires relatively stiff materials, which facilitate the differentiation pathway of undifferentiated cells into the osteocyte lineage. Organically-modified ceramic (Ormocer®) materials are popular materials for orthopaedic applications. For example, the zirconium–silicon based hybrid sol-gel photopolymer (ORMOSIL SZ2080) has been used for orthopaedic applications due to its biocompatibility; 1% w/w ethyl Michler's ketone is a popular photoinitiator for use with this polymer. Extensive washing is commonly used to remove the unreacted monomer and the photoinitiator. Human adipose- and bone marrow-derived stem cells have been grown on this material in three-dimensional scaffold<sup>40</sup> (Figure 5) and two-dimensional textured surface<sup>41</sup> formats to examine the effect of scaffold geometry on osteogenic differentiation.

2PP is a unique tool to perform additive manufacturing for biological applications since structures of arbitrary geometry on the size scale of the cell or of sub-cellular structures can be reliably reproduced. Due to the fabrication speed limitations of 2PP, the most promising current applications of 2PP have been for *in vitro* assays that examine cellular behavior rather than for implantable tissue engineering scaffolds.

#### Optics considerations

The 2PP apparatus is used to (a) tightly focus the laser into the sample while allowing for cleaning or shaping of the beam and (b) translate the focal point within the sample. Titanium:sapphire lasers are the most commonly used for 2PP experiments; however, other types of femtosecond lasers (e.g. frequency doubled Nd:glass lasers) or picosecond lasers may be used for 2PP. The most simple 2PP setup consists of a laser source, a focusing objective, a translational stage, a laser power control system, and a shutter; most of these components are also found on microscopes. As such, building a 2PP system on an existing two-photon fluorescence microscope is commonly undertaken. Additions to the setup can improve the resolution and fabrication speed. Using the scanning mirrors as the primary method for moving the laser focus results in orders of magnitude faster fabrication versus using the translational stages (although this approach is limited to the field of view of the objective). Controlling the group velocity dispersion using optics such as prism compressors or chirped mirrors can reduce the pulse duration; with a shorter pulse duration, 2PP threshold intensities can be achieved with lower average laser power values. An example 2PP beam path is given in Figure 6, which contains all of the aforementioned components.

Use of a spatial light modulator (SLM) is similar to use of projection SLA in that the beam is shaped to present more than a one-dimensional point for fabrication. Unlike ultraviolet lithography, in which the projection of any two-dimensional image will suffice, manipulating a three-dimensional focal volume is more challenging from hardware and computational standpoints. While a two-dimensional mask suffices for ultraviolet illumination, amplitude and phase modulation within the beam must be manipulated to form the desired voxel shape for projection of a three-dimensional image. This parameter is achieved by inserting a mask within the 4f system Fourier plane, the plane in between the two lenses. The simplest case would be a pinhole spatial filter, in which low spatial frequencies that focus closer to the optical axis are allowed through. Computer-controlled SLMs placed at the first conjugate plane can introduce phase delays within certain regions of the beam. Currently available SLMs are essentially small liquid crystal displays and are usually controlled via a Digital Visual Interface (DVI) input; instead of controlling the color intensity, each pixel on this device changes the phase of the incident light. The current approach is to generate a holographic image, which generates the desired pattern after a Fourier transformation. Many algorithms are available, including *ab initio* ones; in general, the highest precision will

be obtained using iterative algorithms. One example of the image generation capabilities of the SLM utilized the Gerchberg-Saxton (GS) iterative algorithm combined with the angular spectrum method to allow for faster calculation of images that deviated from the focal plane. One stated limitation of this approach is that the out-of-focus light from one component image was visible at the focus of another component image. For 2PP, this limitation is not consequential since the photopolymer is transparent to the unfocused light. As shown in Figure 7, Hilario et al. projected different letters that were each independently mobile in all three axes.<sup>42</sup>

Using a SLM for 2PP is currently limited by the need to provide sufficient laser power that initiates polymerization. When projecting a point source, a 1 µm voxel requires only a couple milliwatts of power and nanoseconds of exposure. Illuminating a 10 µm cubic region would require on the order of watts of power, which would be difficult to achieve considering that this amount of power is the entire power of many currently available titanium:sapphire lasers; in addition, significant power loss is associated with the spatial light modulator and other elements in the beam path. Yang et al. generated structures using two-dimensional projections in a layer-by-layer fashion; this approach involved 560 mW of power and multiple seconds of exposure. Three-dimensional 2PP was utilized to produce a tetrahedron; multiple point foci mobile in all three dimensions were used to create this structure. Making a three-dimensional structure using only solid-state hardware means that it is theoretically possible to project an entire structure instead of a single layer (as with a two-dimensional projection). This technology is limited by both laser power and current hologram generation capabilities; however, useful applications of this currently incomplete technology have been described. For example, Gittard et al. utilized multiple static foci, which were scanned separately by a galvanoscanner, to produce multiple structures in parallel. Additionally, four ring-shaped unit cells (Figure 8) of a tissue engineering scaffold were produced simultaneously from polyethylene glycol diacrylate; this structure was geometrically identical to one fabricated using a single-beam approach. In addition, an array of thirty-six rocket-shaped microneedles was produced from an Ormocer® material using a multibeam approach.

## Conclusions

Several innovations involving the use of 2PP for biological applications have been described in recent years. Many recent studies have drawn from techniques and materials that were originally utilized in more well-established lithographic techniques. Although many bulk polymers that are commonly utilized in lithographic techniques are not toxic, the unreacted monomers, oligomers, and photoinitiators can present biocompatibility issues; extensive post-2PP washing is commonly used when processing photopolymers that were not designed for biomedical applications. The precise geometrical requirements for medical devices and the often toxic chemistries used in photopolymerization are unique challenges for 2PP. Biocompatible photopolymers have been synthesized from biological polymers such as chitosan and gelatin; these materials have been polymerized using novel photoinitiator designs that were formulated for a large TPA cross-section and for water solubility. Advances in the mechanical/optical side have primarily focused on increasing the fabrication speed to address the commercial and clinical requirements for higher throughput.

Despite the unique opportunities that it offers for biological applications, 2PP technology has yet to sufficiently distinguish itself from incumbent technologies. Since it utilizes materials and technologies that were originally developed for other fields, an interdisciplinary approach is required to utilize 2PP technology for biological applications. Since tissues require specific physical, chemical, and geometrical conditions to perform their intended functions, biologists must collaborate with polymer chemists to design polymers that exhibit appropriate biological properties. The development of photoinitiators with higher TPA efficiency is also needed. Optimizing the laser beam path for throughput rather than for high resolution processing requires an intimate knowledge of optics for modulating the laser at great angular deviations, in which the paraxial approximation cannot be used to achieve a large build volume. SLMs promise to be a key component in 2PP technology but must overcome several limitations, such as the low pixel fill factor that introduces unintended spatial frequencies into the beam. In addition, software and algorithms to run the SLM need to be improved to obtain real-time hologram generation. Calculating the phase and amplitude deviations within a beam to project the

desired three-dimensional image of an arbitrary structure is far removed from engineering the cellular environment or other biological applications. The individual components of a biologically-relevant 2PP system have been published; however, to this point, a single system that is capable of processing biocompatible materials on the centimeter-scale with sub-micrometer resolution has yet to be demonstrated.

#### References

- 1. Emons, M., et al., Opt Mater Express (2012) 2 (7), 942
- 2. Wu, D., et al., Light-Sci Appl (2015) 4
- 3. Hjorto, G. M., et al., Biomed Microdevices (2015) 17 (2)
- 4. Miller, P. R., et al., Adv Healthc Mater (2014) 3 (6), 876
- 5. Turunen, S., et al., Opt Laser Eng (2014) 55, 197
- 6. Marino, A., et al., Acta Biomater (2014) **10** (10), 4304
- 7. Gittard, S. D., et al., J Diabetes Sci Technol (2009) 3 (2), 304
- 8. Koroleva, A., et al., Biofabrication (2012) 4 (1)
- 9. Malinauskas, M., et al., Opt Express (2010) 18 (10), 10209
- 10. Ong, B. H., et al., Opt Lett (2006) 31 (10), 1367
- 11. Seet, K. K., et al., Appl Phys Lett (2006) **89** (2)
- 12. Baldacchini, T., et al., Opt Express (2012) 20 (28), 29890
- 13. Waller, E., and von Freymann, G., *Polymers-Basel* (2016) **8** (8), 297
- 14. Sheikbahae, M., et al., Ieee J Quantum Elect (1990) 26 (4), 760
- 15. Ajami, A., et al., J Opt Soc Am B (2010) 27 (11), 2290
- 16. Cumpston, B. H., et al., Nature (1999) 398 (6722), 51
- 17. Pawlicki, M., et al., Angew Chem Int Edit (2009) 48 (18), 3244
- 18. Aydin, M., et al., Macromol Rapid Comm (2003) 24 (12), 718
- 19. Nazir, R., et al., Chem Mater (2014) 26 (10), 3175
- 20. Orellana, B., et al., Macromolecules (1999) 32 (20), 6570
- 21. Nguyen, A. K., et al., Regen Med (2013) 8 (6), 725
- 22. Li, Z. Q., et al., Rsc Adv (2013) 3 (36), 15939
- 23. Pawar, A. A., et al., Sci Adv (2016) 2 (4), e1501381
- 24. Song, L., et al., Dent Mater (2016) 32 (1), 102
- 25. Denis, A. B., et al., Journal of Spectroscopy (2016) 2016, 1
- 26. Salgado, V. E., et al., Int J Adhes Adhes (2017) 72, 6
- 27. Randolph, L. D., et al., Dent Mater (2016) 32 (2), 136
- 28. Cicha, K., et al., J Appl Phys (2011) **110** (6)
- 29. Kufelt, O., et al., Acta Biomater (2015) 18, 186
- 30. Kufelt, O., et al., Biomacromolecules (2014) 15 (2), 650
- 31. Van den Bulcke, A. I., et al., Biomacromolecules (2000) 1 (1), 31
- 32. Ovsianikov, A., et al., Materials (2011) 4 (1), 288
- 33. Koroleva, A., *et al.*, *Biofabrication* (2012) **4** (2)
- 34. Kloxin, A. M., et al., Nat Protoc (2010) 5 (12), 1867
- 35. Mastropasqua, L., Eye Vis (Lond) (2015) 2, 19
- 36. Kuetemeyer, K., et al., Opt Express (2011) 19 (17), 15996
- 37. Kaehr, B., et al., Anal Chem (2006) 78 (9), 3198
- 38. Kaehr, B., and Shear, J. B., *P Natl Acad Sci USA* (2008) **105** (26), 8850
- 39. Khripin, C. Y., et al., Soft Matter (2010) 6 (12), 2842
- 40. Koroleva, A., et al., Plos One (2015) 10 (2)
- 41. Skoog, S. A., et al., Biointerphases (2014) 9 (2)
- 42. Hilario, P. L., et al., Opt Lett (2014) **39** (7), 2036
- 43. Yang, L., et al., Opt Commun (2014) **331**, 82
- 44. Zalesskii, A. D., et al., Russ J Phys Chem B+ (2012) 6 (3), 357
- 45. Gittard, S. D., et al., Biomed Opt Express (2011) 2 (11), 3167
- 46. Lin, C. Y., et al., Opt Express (2012) 20 (13), 13669

### Figure Captions

- Figure 1 (Color online) Z-scans for rhodamine B were carried out with the same pulse energy at several pulse widths. Circles represent experimental data that were obtained with 100 fs pulses and squares represent experimental data that were obtained with 25 fs pulses. Reprinted from Reference <sup>15</sup>.
- Figure 2 Structures of new 2PA photoinitiators and reference compounds. Reprinted (adapted) with permission from Nazir, R., Danilevicius, P., Ciuciu, A. I., Chatzinikolaidou, M., Gray, D., Flamigni, L., Farsari, M., Gryko, D. T. (2014). π–expanded ketocoumarins as efficient, biocompatible initiators for two-photon-induced polymerization. *Chemistry of Materials*, *26*(10), 3175-3184. doi: 10.1021/cm500612w Copyright 2014 American Chemical Society.
- Figure 3 a) Merged live/dead staining after five days of culture for a 50% polyethylene glycol diacrylate-riboflavin-triethanolamine scaffold seeded with endothelial cells. b) polyethylene glycol diacrylate exhibits red autofluorescence; ethidium homodimer-1 (dead cell) fluorescence is distinct from the polyethylene glycol diacrylate fluorescence. Republished with permission of Future Medicine Ltd, from "Two-photon polymerization of polyethylene glycol diacrylate scaffolds with riboflavin and triethanolamine used as a water-soluble photoinitiator." Nguyen, A. K., et al. Vol. 8 (6), 2011; permission conveyed through Copyright Clearance Center, Inc. Figure 4 (a) Processing windows of investigated initiators in TPIP screening tests; (b) Classifications of the structures by the typical quality of their shapes. Republished with permission of Royal Society of Chemistry, from "Initiation efficiency and cytotoxicity of novel water-soluble two-photon photoinitiators for direct 3D microfabrication of hydrogels." Li, Z. Q., et al. Vol. 3 (36), 2013; permission conveyed through Copyright Clearance Center, Inc.
- Figure 5 Cells on scaffolds after 21 days in osteogenic and control cultures: (a and c) human adipose derived stem cells and human bone marrow stromal cells from osteogenic culture; (e and g) human adipose derived stem cells and human bone marrow stromal cells from control culture. High magnification images showing calcium phosphate deposits of human adipose derived stem cell and human bone marrow stromal cell cultures on Zr-Si scaffolds in osteogenic (b and d) and control (f and h) conditions; (i-l) Energy-dispersive X-ray spectroscopy mapping confirming the presence of calcium and phosphorus in the accumulations. Scale bars: (a, c, e, g) 60 μm, (b, d, f, h) 5 μm, (i) 50 μm and (j-l) 10 μm. Reprinted from Reference <sup>40</sup> licensed under Attribution 2.0 Generic (CC BY 2.0). Figure 6 Optical setup of a femtosecond laser imaging and microfabrication system, which is capable of fluorescence lifetime imaging microscopy. Reprinted from Reference <sup>46</sup>.
- Figure 7 Experimental generation of arbitrary light fields using one proposed method. The size is approximately 4.8 mm. Reprinted from Reference <sup>42</sup>.
- Figure 8 Tissue engineering scaffolds made by 2PP with single focus structuring (a) and four foci structuring (b). Image of bovine endothelial cells growing on scaffold made by multi-beam 2PP (c). Reprinted from Reference <sup>45</sup>.

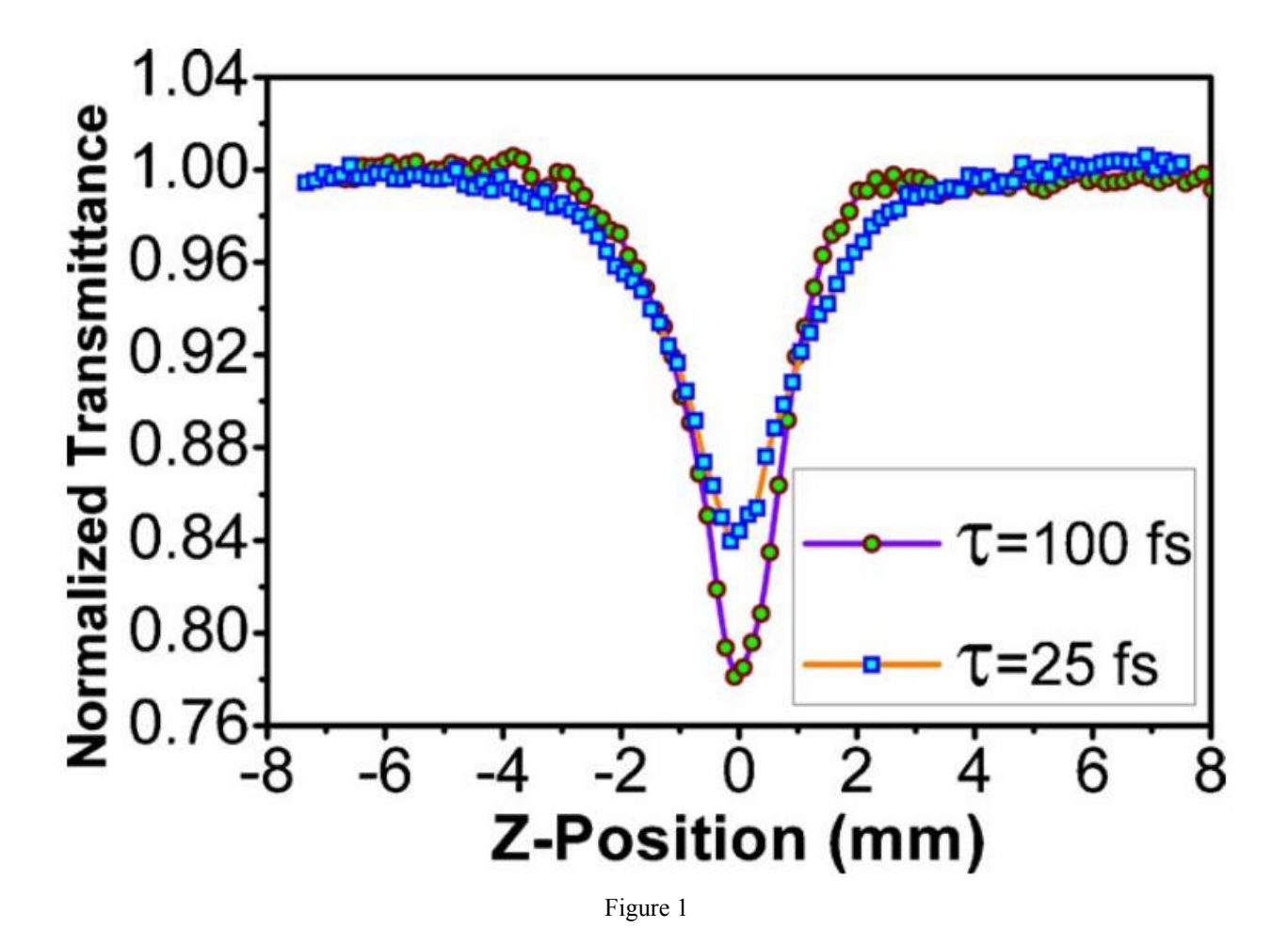


Figure 2

М

R

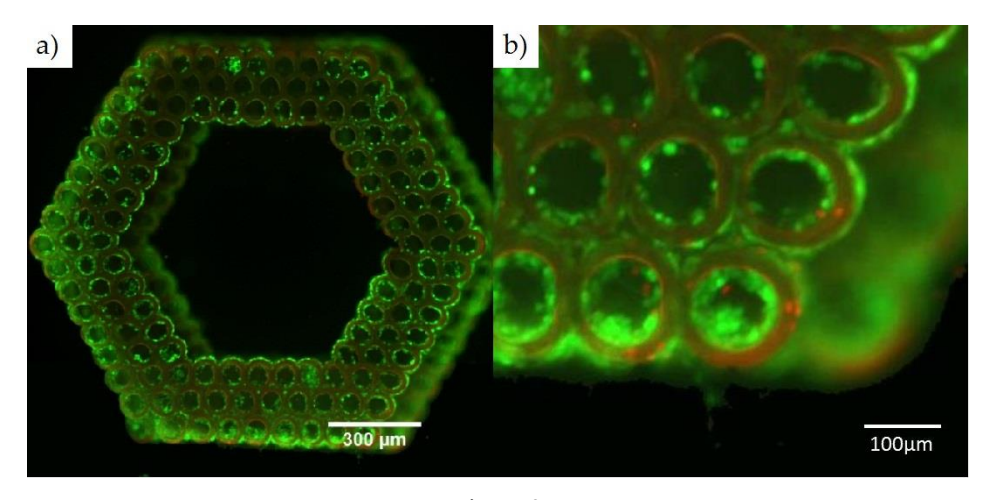


Figure 3

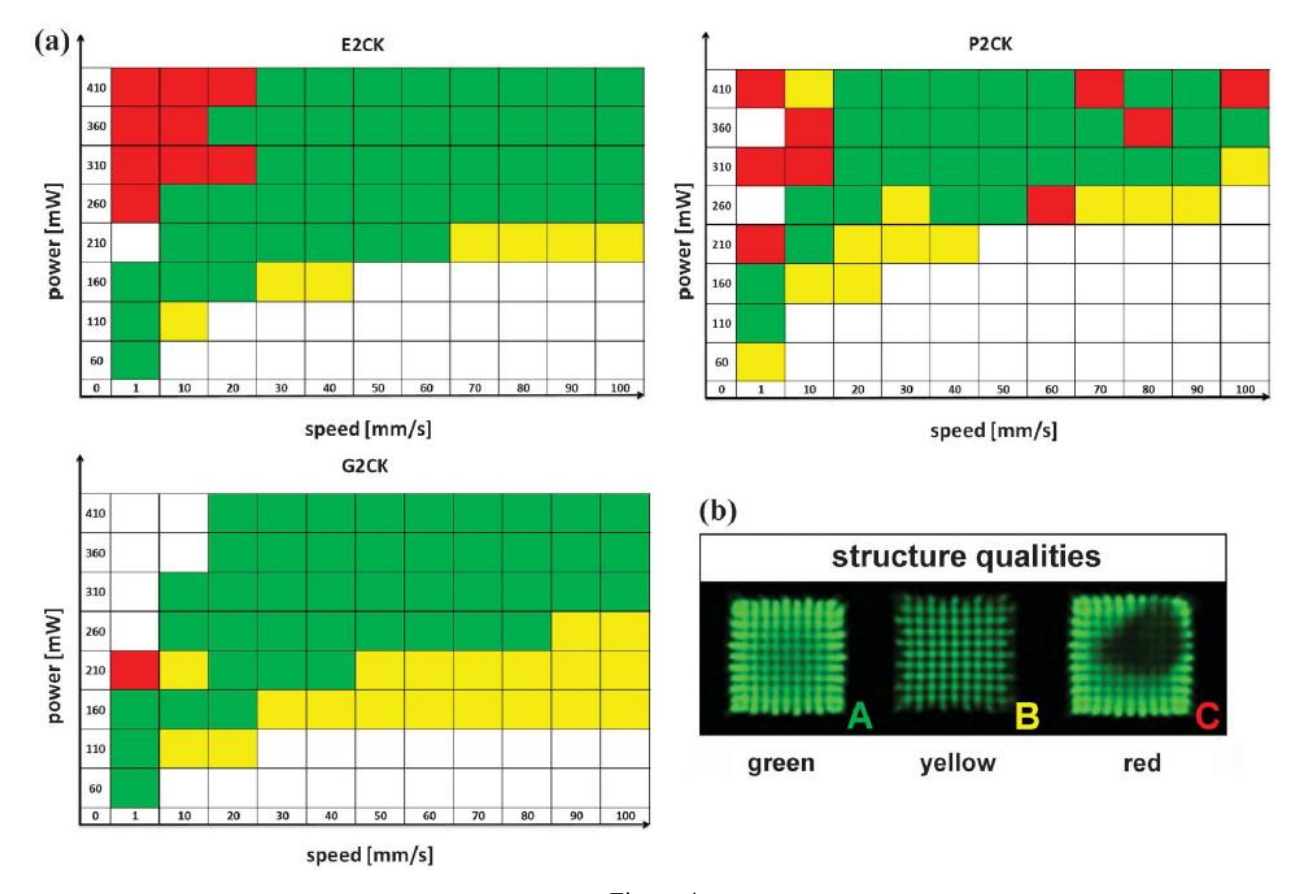


Figure 4

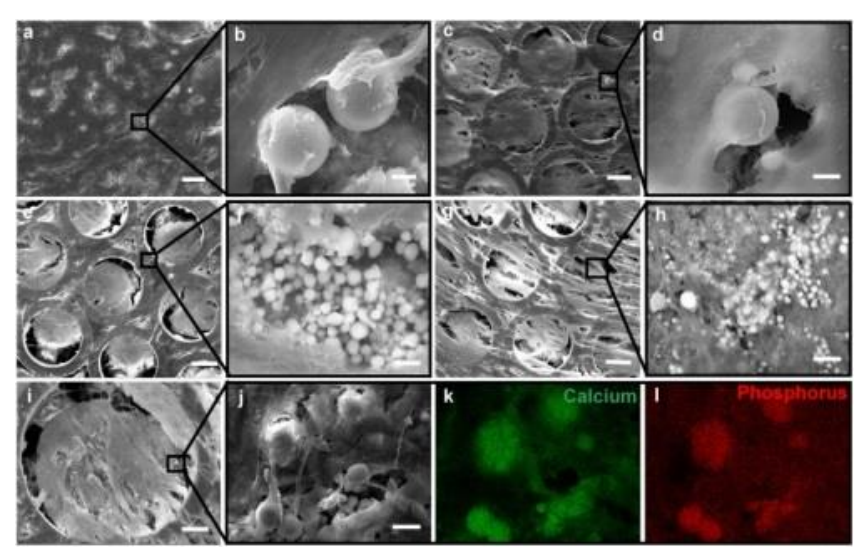
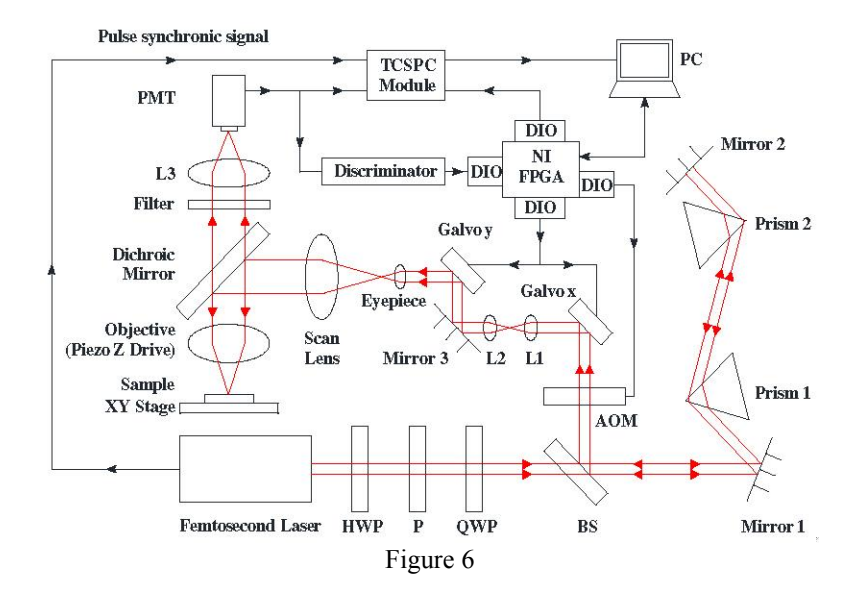


Figure 5



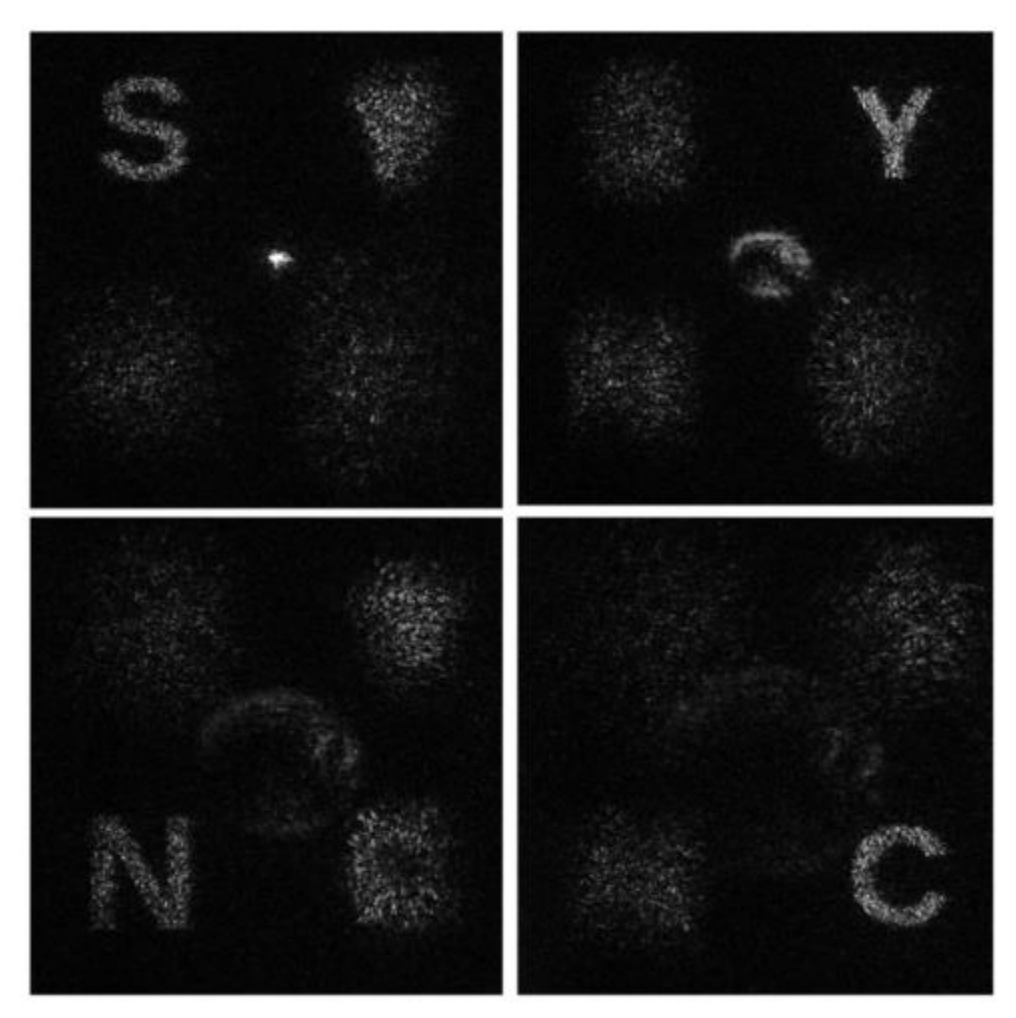


Figure 7

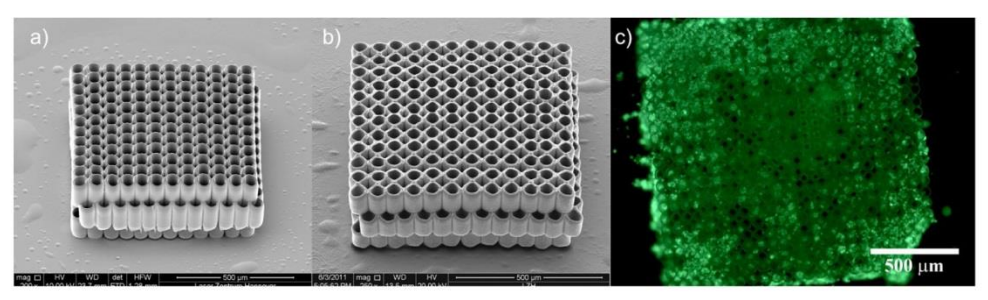


Figure 8